Desalination and Water Treatment
www.deswater.com

doi: 10.5004/dwt.2019.23726

150 (2019) 348–360
May

Adsorption of acid blue 25 from aqueous solution using zeolite and surfactant modified zeolite

L. Sivarama Krishna[a,b,*], K. Soontarapa[a,b,*], Nabel Kalel Asmel[c], Mohammad Alamgir Kabir[d,e], Ali Yuzir[f], W.Y. Wan Zuhairi[d], Y. Sarala[g]

[a]*Department of Chemical Technology, Faculty of Sciences, Chulalongkorn University, Pathumwan, Bangkok, 10330, Thailand, emails: svurams@gmail.com (L. Sivarama Krishna), Khantong.S@chula.ac.th (K. Soontarapa)*
[b]*Center of Excellence on Petrochemical and Materials Technology, Chulalongkorn University, Pathumwan, Bangkok, 10330, Thailand*
[c]*Building and Construction Technology Engineering, Northern Technical University, 41002 Mosul, Iraq, email: nabeelasmeel@yahoo.com*
[d]*Geological Survey of Bangladesh, 153, Pioneer Road, Segunbagicha, Dhaka-1000, Bangladesh, emails: kabirgsb@gmail.com (M.A. Kabir), wanzuhairi@yahoo.com (W.Y. Wan Zuhairi)*
[e]*Geology program, School of Environmental Science and Natural Resources, FST, University Kebangsaan Malaysia, Bangi-43600, Selangor, Malaysia*
[f]*Department of Environmental Engineering and Green Technology (EGT), MJIIT- Universiti Teknologi Malaysia, Jalan Sultan Yahya Petra, 54100 Kuala Lumpur, email: muhdaliyuzir@utm.my*
[g]*Department of Chemistry, Chaitanya Bharathi Institute of Technology, Gandipet, Hyderabad 500 075, India, email: saralayaaratha@yahoo.com*

Received 17 April 2018; Accepted 31 December 2018

ABSTRACT

In the present study, we have demonstrated the Indonesian natural zeolite and modified zeolite was used to remove the acid blue 25 (AB25) from wastewater. The adsorption capacity of AB25 on zeolite and modified zeolite (zeolite-CTAB) were investigated by various batch adsorption experiments. The modification effect on the surface of zeolite was analyzed using Fourier transforms infrared spectra, scanning electron microscopy, energy-dispersive X-ray spectroscopy, X-ray fluorescence, and X-ray diffraction, respectively. The maximum removal of AB25 was obtained under acidic conditions at pH 2. The kinetic experimental results imply that the adsorption of AB25 onto these adsorbents well followed the second-order kinetic model. The maximum adsorption capacity of 64.2 mg/g was found in Zeolite at 30°C and 112.44 mg/g for zeolite-CTAB at 60°C. The results revealed that the adsorption of AB25 onto zeolite-CTAB fitted better to Langmuir model and Zeolite fitted better with Freundlich model. The AB25 adsorption on zeolite-CTAB increases with an increasing temperature indicates that the preferential adsorption may occur at a higher temperature. The positive value of $\Delta H°$ in zeolite-CTAB material thermodynamic parameters indicates that the process was an endothermic process. These results indicate that zeolite-CTAB has high adsorbent efficiency and it is promising adsorbents for removing the dye AB25.

Keywords: Zeolite; Zeolite-CTAB; Acid Blue 25; Adsorption; Wastewater

* Corresponding authors.

1. Introduction

The dye containing effluents from the textile dyeing industries released a large amount of colored wastewater into the aquatic environment. These highly colored wastewaters contain various kinds of synthetic dyestuffs and heat or hot, with alkaline in nature, besides it also contains a high quantity of dissolved solids [1,2]. These types of dyes used in the industries include cationic (basic dyes), anionic (direct, acid, and, reactive dyes), and non ionic dyes. Acid dyes are the most problematic due to their bright color, acidic nature, water-soluble, and reactive characteristics. Nevertheless, so far very few research works has been focused on adsorption of acidic dyes [3].

Synthetic dyes are non-biodegradable and highly visible even if present in small amount in water, because they contains an aromatic complex structures, which lead to the influences aesthetic merit and decrease the light penetration needed for photosynthesis and thus these dyes ultimately disturb aquatic ecosystem [4–6]. Some of the dyes decompose into carcinogenic aromatic amines under anaerobic conditions and cause serious health problems to human beings as well as the aquatic environment and other animals. Many dyes and their by products break down into different products which are toxic for living organisms [7–9]. Conventional biological wastewater treatment processes are not efficient in treating dyes present in wastewater. Hence, the elimination of dyes from the wastewater accepted environmental importance [10].

Many approaches have been developed for decontamination of water, e.g., precipitation, adsorption, filtration, coagulation, oxidation and membrane separation, respectively. However, the adsorption is known to be one of the most effective techniques [11,12]. However, high cost has led in seeking for low-cost adsorbents. New, economical, locally available and highly effective adsorbents are still in the process of development.

Zeolites are highly porous aluminosilicates with different cavity structures. Their structures consist of a three-dimensional framework, having a negatively charged lattice. Zeolite possess permanent negative charges in their crystal structure making them suitable for surface modification using cationic surfactants in which each molecule composed of hydrophilic and positively charged head group. The negative charge is balanced by cations which are exchangeable with certain cations in solutions. The characteristics and applications of zeolites have been reviewed [13]. High ion-exchange capacity and relatively high specific surface areas, and more importantly their relatively low prices make zeolites attractive adsorbents.

In the present study, zeolite has been modified by cationic surfactant cetyltrimethylammonium bromide (CTAB) resulting to develop the zeolite-CTAB and to enhance the acid blue 25 (AB25) adsorption capacity of zeolite for acidic dye AB25. The influence of pH, temperature, initial dye concentration, and dose effect on the adsorption are investigated. In addition, the equilibrium has been investigated in batch method. Zeolite and zeolite-CTAB were characterized using various characterization tools such as Fourier transform infrared spectroscopy (FT-IR), scanning electron microscopy (SEM), energy-dispersive X-ray spectroscopy (EDX), X-ray fluorescence (XRF) and X-ray diffraction (XRD). The adsorption capacity for the removal of AB25 was determined.

2. Materials and methods

2.1. Materials

The natural zeolite material was obtained from Indonesia, and extensively investigated for dye removal. It was crushed and ground fine powder. The CTAB (99.3%) and AB25 (45%) dye were purchased from Sigma-Aldrich Company, Ltd (Australia) and used without further purification.

2.2. Preparation of cationic surfactant modified Zeolite (Zeolite-CTAB)

For surfactant modification of zeolite the material was first ground well, and the powder was then dried in an oven for 12 h. Then 20 g of dried material and 2 g of CTAB was placed in a 500 mL Erlenmeyer flask and then mixed with 400 mL of double distilled water. The reaction components were then stirred with the help of a rotary shaker for 24 h at 200 rpm. The obtained product was filtered and washed repeatedly with distilled water. Further, the washed sample was then dried in the oven at a temperature of 55°C for 12 h, the dried modified sample was grounded and stored in an airtight container (desiccators) for further use. The prepared sample has been abbreviated as zeolite-CTAB.

2.3. Characterization of materials

The types of functionalities of the materials and adsorbed species were determined by infrared spectroscopy. The Fourier transforms infrared (FT-IR) spectra of zeolite, zeolite-CTAB, and AB25 loaded zeolite-CTAB were recorded in the range of 4,000–400 cm^{-1} using Spectrum BX FT-IR system (Model no. Perkin Elmer/BX HO22154) to confirm the surface modification of zeolite. Particle morphology was observed by SEM at 1,000 magnifications (Model: Zeiss Supra 55 VP, Germany). The mineral composition was analyses through the elemental analysis and recording of the EDX spectroscopy image of zeolite, zeolite-CTAB, and AB25 loaded zeolite-CTAB was carried out using an energy dispersive X-ray spectrometer attached to a SEM. The analysis of mineral or chemical compositions except all organic components was performed using XRF (Bruker S8 Tiger). The phases of the samples were determined by XRD (Bruker AXS Germany and model: D8 Advance).

2.4. Point of zero charges (pH_{PZC})

The zero surface charge characteristics of the zeolite and zeolite-CTAB were determined using the solid addition method. Fourth mL of 0.1 M KNO_3 solution was transferred to a series of 100 mL stopper conical flasks. The pH_i values of the solutions were roughly adjusted between 2 and 12 by adding either 0.1 N HCl or 0.1 N NaOH and were measured by using pH meter (HI 2211 pH/ORP meter). The total volume of the solution in each flask was exactly adjusted to 25 mL by adding a KNO_3 solution of the same strength. The pH_i values of the solutions were then accurately noted.50 mg

of each zeolite and zeolite-CTAB was added separately to each flask, and the flask was securely capped immediately. The suspensions were then kept under shaking condition for 24 h. The final pH values of the supernatant liquid were noted. The difference between the final pH (pH_f) and initial pH (pH_i) values (ΔpH) was plotted against the pH_i. The point of intersection of the resulting curve with abscissa, at which pH_0, gave the pH_{PZC}.

2.5. Adsorption experiments

To study the effect of variables like initial concentration, temperature, adsorbent dosage, and pH for the removal of AB25, a batch experiments were carried out in a 50 mL screw type Erlenmeyer flask and the sample was placed in a shaker with a constant speed of 200 rpm at room temperature (25°C ± 1°C). The effect of zeolite and zeolite-CTAB doses and their optimal amount for the adsorption of AB25 was obtained by taking 10 different amount of zeolite and zeolite-CTAB (10–100 mg) and agitated in the rotary shaker (Protech-orbital Shaker, Model-719) at 200 rpm for 120 min with 50 mg/L solution of AB25 at original pH of 6.37. The effect of pH on the adsorption of AB25 on zeolite and zeolite-CTAB has been studied over a pH range of 2–12. The pH of the dye solution was adjusted with 0.1 M HCl and 0.1 M NaOH. In this study, 25 mL of a fixed initial concentration (100 mg/L) of AB25 at different pH were agitated with 50 mg of each zeolite and zeolite-CTAB in the rotary shaker at 200 rpm for 120 min. The effect of initial dye concentration and contact time on the adsorption of AB25 on zeoliote and zeolite-CTAB was studied for different AB25 concentrations at different time intervals. In this study, 50 mg of each zeolite and zeolite-CTAB was added to 25 mL AB25 solutions of four different concentrations in the 50 mL screw type Erlenmeyer flasks and the mixtures were then agitated in the rotary shaker for 5, 10, 20, 30, 45, and 60 min. To understand the effect of temperature on the influence of the removal of AB25 by zeolite and zeolite-CTAB, experiments were conducted at different temperatures of 30°C, 40°C, 50°C, and 60°C for different AB25 concentrations (25–125 mg/L) at pH 2. In this study, 50 mg of each zeolite and zeolite-CTAB adsorbent was added to the dye, AB25 of each five different concentrations in the 50 mL screw type Erlenmeyer flasks. And it was then instantly agitated in the temperature controlled Innova 4,200 incubator shaker at 200 rpm for 60 min. These samples were taken out from the shaker at pre-determined time intervals for kinetics study and the dye solution was separated from the adsorbents by centrifugation in the Sigma laboratory centrifuges-Sartorius machine at 3,000 rpm for 10 min. The absorbance of supernatant solutions was measured spectrophotometrically by monitoring the absorbance at 610 nm using spectrophotometry, model: HeλIOSγ from which the concentration of AB25 was determined and the amounts of AB25 adsorbed on the adsorbents were obtained. The pH of the AB25 solution was measured using pH meter (Model: HI 2211).

The amount of AB25 adsorbed on the surface of the adsorbent at time t, q_t (mg/g) was calculated using a mass balance equation.

$$q_t = [(C_0 - C_t)]\, V/W \tag{1}$$

C_o and C_t (mg/L) are the initial concentration and concentration at time t, respectively; V is the volume of the solution (L), and W is the mass of dry adsorbent used (g).

The dye removal percentage was calculated as follows:

$$\text{Removal percentage} = (C_0 - C_e)/C_e \times 100 \tag{2}$$

where C_e is the equilibrium concentration in solution (mg/L).

3. Theory of adsorption kinetics and isotherms

3.1. Kinetic models

In order to explore the mechanism of adsorption, characteristic constants were perverse with two commonly used kinetic models Pseudo-first order (PFO) model (Eq. (3)) [14], and pseudo-second order (PSO) model (Eq. (4)) [15] applied to determine the rate of the adsorption process besides providing valuable information. The nonlinear form of the PFO kinetic model is given as follows:

$$q_t = q_e\left(1 - \exp\left(-K_1 t\right)\right) \tag{3}$$

PSO equation predicts the behavior over the whole range of adsorption. The nonlinear form of the PSO kinetic model is given as follows:

$$q_t = \frac{K_2 q_e^2 t}{\left(1 + q_e K_o t\right)} \tag{4}$$

where k_1 (1/min) is the rate constant of PFO adsorption, k_2 (g/mg. min) is the rate constant of PSO adsorption. q_e is the amount of dye adsorbed on adsorbent at equilibrium and q_t is the amount of dye adsorbed on adsorbent at time t.

3.2. Adsorption isotherms

Adsorption isotherms predict the relationship between adsorbate and adsorbent in solution when both the phases are in equilibrium with each other. Langmuir isotherm predicts the homogenous and monolayer adsorption onto the adsorbent surface. The adsorption data obtained was applied to Langmuir and Freundlich models to analyze the data which are widely used in solid-liquid adsorption systems. Langmuir isotherm model is represented by the following equation [16]:

$$q = \frac{K_L q_m C_e}{1 + K_L C_e} \tag{5}$$

where q is the quantity of adsorbed AB25 at equilibrium settings (mg/g), C_e represents the AB25 equilibrium concentration in solution (mg/L), q_{max} is the maximum adsorption capacity of adsorbent (mg/g) and K_L is the Langmuir constant related to the adsorption energy (L/mg).

R_L, a dimensionless constant, is used to determine whether adsorption is favorable or not and this was calculated by as follows:

$$R_{L1} = \frac{1}{1 + K_L C_0} \quad (6)$$

where C_0 is the initial concentration of dye (mg/L).

Freundlich isotherm model is also applied to describe the adsorption of dye. This isotherm is an empirical equation employed to describe the heterogeneous system. Freundlich isotherm model equation is represented by [17]:

$$q = K_f C_e^{\frac{1}{n}} \quad (7)$$

where K_f is the Freundlich constant, and '1/n' is the heterogeneity factor. All remaining parameters of Langmuir and Freundlich isotherm models have different isotherm constant that were determined using nonlinear regression of the experimental data utilizing excel-solver software.

3.3. Thermodynamic parameters

Thermodynamic parameters can be calculated from the difference of the thermodynamic distribution coefficient, K_L with a change in temperature. The standard free energy change, $\Delta G°$, will be calculated using the following expression [18–20]:

$$\Delta G° = -RT\ln Kd \quad (8)$$

$$\Delta G° = \Delta H° - T\Delta S° \quad (9)$$

where K_d is the procured by multiplying Langmuir constant b. R is the universal gas constant (8.314 J/K. mol), and T is the temperature in Kelvin.

Standard enthalpy ($\Delta H°$) and entropy ($\Delta S°$) of adsorption can be estimated from Van't Hoff equation:

$$\ln K_d = (-\Delta H°/RT) + S°/R \quad (10)$$

$$K_d = b(L/g) \times MW(\text{g/mol}) \quad (11)$$

4. Results and discussion

4.1. Characterization of zeolite and zeolite-CTAB

FT-IR spectra of natural zeolite and zeolite-CTAB are depicted in Fig. 1. The FT-IR spectrum of zeolite-CTAB shows two pronounced adsorption bands at around 2,851 and 2,922 cm^{-1}, which can be attributed to the asymmetric and symmetric stretching vibrations of $–CH_2$ and $–CH_3$ respectively, it indicates that the presence of a long alkyl chain in the Zeolite-CTAB and supports the modification of zeolite with CTAB. These peaks are confirmed by another work [21]. Strong bands both for zeolite and zeolite-CTAB centered at 1,010 and 1,100 may be belonged to Si-O terminal vibration together with those at around 491, 626, and 796 cm^{-1} which indicate the bending vibrations and the symmetric stretching vibration of Si-O-Al and Si-O-Si bridge band respectively. Bands at 3,405 and 1,641 cm^{-1} may be due to the presence of bounded hydroxyl OH^- groups and molecular water respectively.

Fourier transforms infrared (FT-IR) spectra of zeolite-CTAB and AB25 loaded zeolite-CTAB are shown in Fig. 2. FT-IR spectra of zeolite-CTAB and AB25 loaded zeolite-CTAB shows that the peak positions of the major bands in the spectrum of dye-loaded zeolite-CTAB is more or less at the same position as in the spectrum of zeolite-CTAB. The spectra of AB25 loaded zeolite-CTAB shows shifting of some peaks to slightly higher frequency, suggesting the involvement of functional groups in the binding of AB25.

4.1.1. Scanning electron microscopy micrographs

The surface of zeolite, zeolite-CTAB, and AB25 loaded zeolite-CTAB was observed by using a SEM. The obtained results are shown in Fig. 3, the natural zeolites are characterized by drusy texture with high porosity, partially developed crystalline laminar habits and conglomerate of compact crystals [22]. The surface morphology of zeolite-CTAB and AB25 loaded zeolite-CTAB is different from that of natural zeolite. The zeolite crystals could not be clearly seen when their surfaces were covered with CTAB and AB25 molecules, confirming that the modification of zeolite with CTAB and loading of AB25 on zeolite-CTAB occurred.

4.1.2. Energy-dispersive X-ray spectroscopy micrographs

EDX spectroscopy images of zeolite, zeolite-CTAB, and AB25 loaded zeolite-CTAB are shown in Fig. 4. The surface

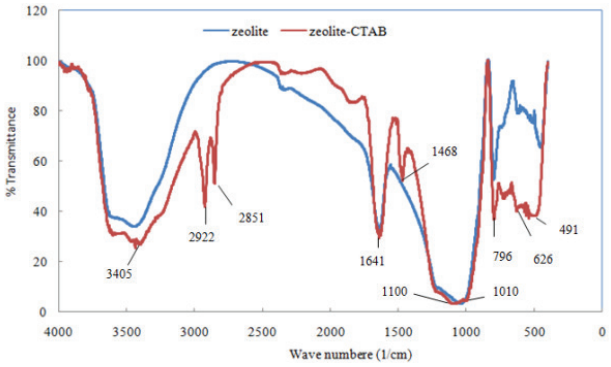

Fig. 1. FT-IR Spectra of zeolite and zeolite-CTAB.

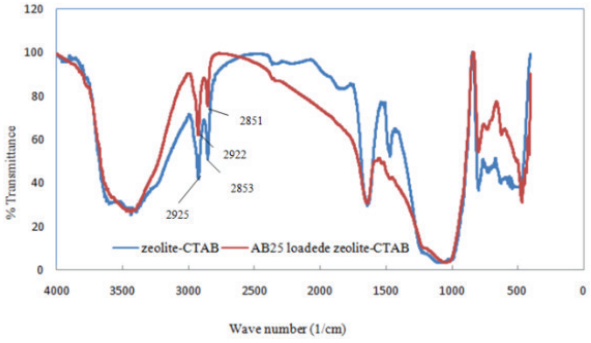

Fig. 2. FT-IR Spectra of Zeolite-CTAB and AB25 loaded Zeolite-CTAB.

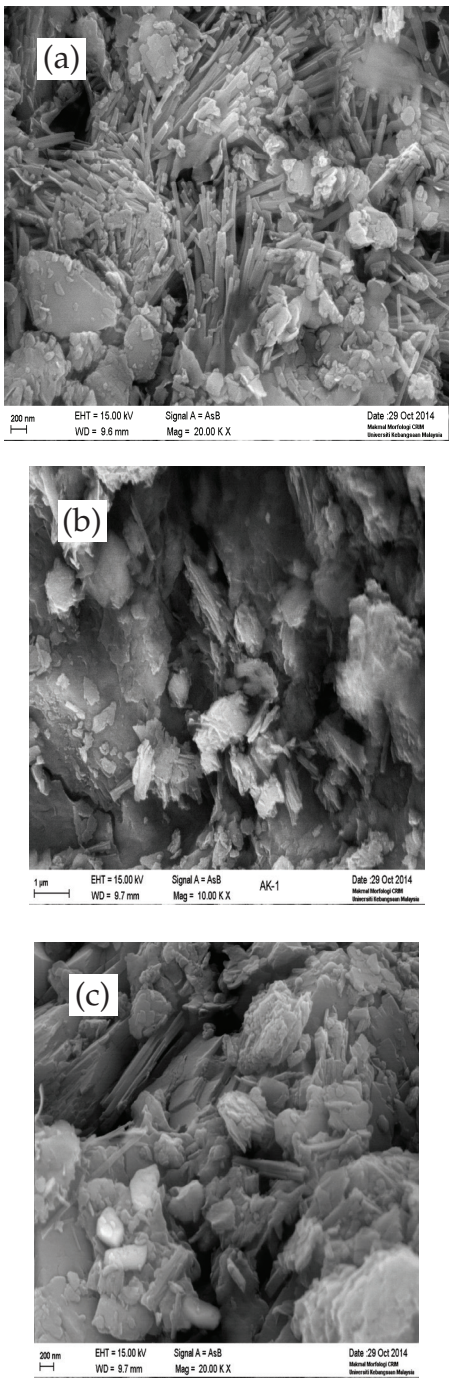

Fig. 3. SEM images of (a) Zeolite, (b) Zeolite-CTAB and (c) AB25 loaded Zeolite-CTAB.

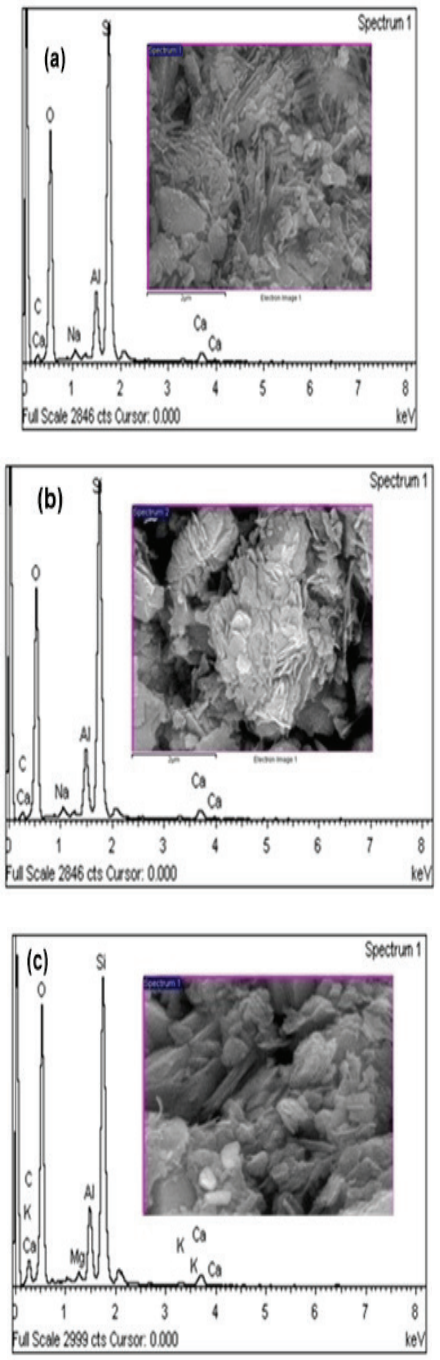

Fig. 4. EDX images with micrographs of (a) Zeolite, (b) Zeolite-CTAB and (c) AB25 loaded Zeolite-CTAB.

morphology of zeolite-CTAB and AB25 loaded zeolite-CTAB are different from that of natural zeolite. Most of the particles in the zeolite show a laminar crystalline characteristic of the phyllosilicate. In the zeolite-CTAB and AB25 loaded zeolite-CTAB these certain particles are less dominated. Intercalation of surfactant molecules and dye molecules in the interlayers generally stand behind the domination of larger laminar crystallites and agglomerates. The zeolite crystals could not be seen clearly when their surfaces were covered with CTAB molecules and AB25, confirming that the modification of zeolite with CTAB has occurred and also the dye has been loaded on the surface of the zeolite-CTAB. The obtained elements from EDX analysis are presented in Table 1. EDX analysis data from Table 1 show that oxygen, silicon, carbon, and aluminum are the major constituent elements along with traces of sodium, calcium, and iron in the form of impurities. Both the weight% and atomic% for carbon has been increased in zeolite-CTAB and AB25 loaded zeolite-CTAB. CTAB has large alkyl chain; we found in zeolite that C% increase from 5.42% (weight) to 10.1%

(weight) in zeolite-CTAB and 13.6% (weight) in AB25 loaded zeolite-CTAB indicating modification of zeolite by CTAB and loading of AB25 in zeolite-CTAB.

4.1.3. X-ray fluorescence analysis

XRF spectroscopy images of zeolite and zeolite-CTAB are shown in Fig. 5. Fifteen oxides and one element (Cl) have been detected from the zeolite through XRF analysis. On the other hand fifteen oxides and one element (Br) have been detected from the zeolite-CTAB through XRF analysis.

This result shows that the major components of zeolite are silica and alumina and the impurities were calcium, iron, sodium, potassium, magnesium, titanium, phosphorous, manganese, and some other oxides. Different compositions with their concentrations are given in Table 2. From the XRF analysis of zeolite and zeolite-CTAB it has been observed that there is no Br peak in the spectrograph of zeolite, but after modification, the Br peak has been observed in the spectrograph of zeollite-CTAB. This peak in the zeolite-CTAB indicates the modification of zeolite was done by CTAB. On the other hand, the Cl peak has been disappeared in the spectrograph of zeollite-CTAB, which may be due to the replacement of Cl by Br and this is possibly due to the modification of zeolite by CTAB.

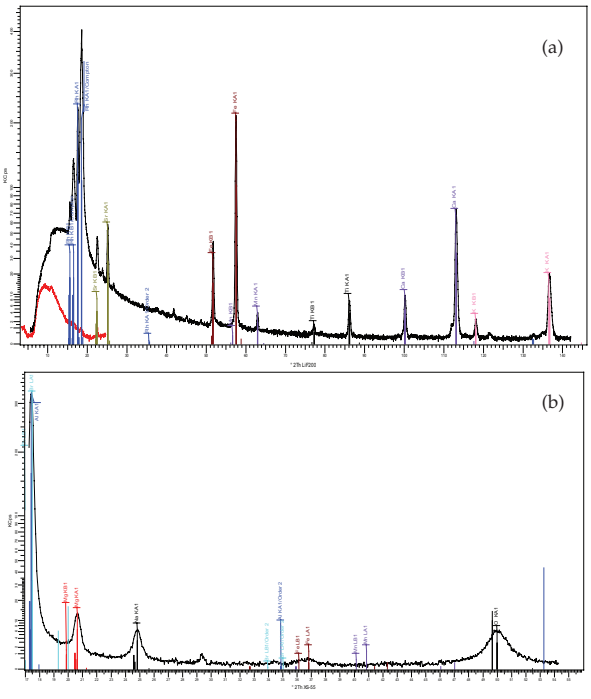

Fig. 5. XRF of (a) Zeolite and (b) Zeolite-CTAB.

4.1.4. X-ray diffraction analysis

XRD analysis of zeolite and zeolite-CTAB samples was done using the software "Eva". Analysis results of the samples are shown in Fig. 6. It can be seen from Figs. 6(a) and (b) that modification of zeolite with CTAB lead to minor structural changes. The quantitative XRD analysis demonstrated that the zeolite consisted of mordenite with other minor constituents of clinoptilolite, quartz, feldspar, etc. The effect of CTAB on zeolite appears at decreasing number of characteristic peaks of mordenite in the zeolite-CTAB because of exchange ions.

Table 2
Composition of zeolite and zeolite-CTAB

Formula	Zeolite composition	Zeolite-CTAB composition
SiO_2	67.8%	65.9%
Al_2O_3	12.0%	11.8%
CaO	3.61%	3.30%
Fe_2O_3	2.18%	2.09%
Na_2O	1.19%	1.06%
K_2O	0.92%	0.96%
MgO	0.84%	0.79%
TiO_2	0.34%	0.33%
P_2O_5	0.05%	0.32%
MnO	0.04%	0.13%
SrO	0.03%	0.04%
SO_3	0.01%	0.03%
ZrO_2	0.01%	0.03%
Cl	0.01%	0.01%
ZnO	59 PPM	51 PPM
CuO	35 PPM	43 PPM

Table 1
Elements from EDX analysis

Zeolite			Zeolite-CTAB		AB25-loaded Zeolite-CTAB	
Element	Weight (%)	Atomic (%)	Weight (%)	Atomic (%)	Weight (%)	Atomic (%)
C K	5.42	8.59	10.1	16.7	13.6	20.1
O K	53.4	63.6	38.4	47.8	54.5	60.1
Na K	0.96	0.79	0.67	0.58	0.57	0.42
Al K	5.46	3.85	6.94	5.12	5.14	3.36
Si K	32.8	22.1	38.8	27.5	24.0	15.1
Ca K	1.96	0.93	3.20	1.59	0.40	0.18
Fe K	–	–	1.83	0.65	1.74	0.77
Totals	100		100		100	

4.1.5. Point of zero charges (pH_{pzc})

Fig. 7 shows the plot between ΔpH and pH_i. The figure points out the point of zero charges for zeolite and zeolite-CTAB. It is obvious from Fig. 7 shows that the surfaces charge of the zeolite and zeolite-CTAB around 6.5 and 6.2, receptively. Hence, the pH_{pzc} at the point of zero charges of the zeolite and zeolite-CTAB is 6.5 and 6.2 respectively. As the pH increases above the pH_{pzc} value, the adsorbent surfaces become predominantly negatively charged, enhancing the electrostatic repulsion between the surfaces of adsorbent and AB25 anions. Similar behavior was reported by the adsorption of Congo red on *Cicer arientinum* Linn fruit shell biomass [7].

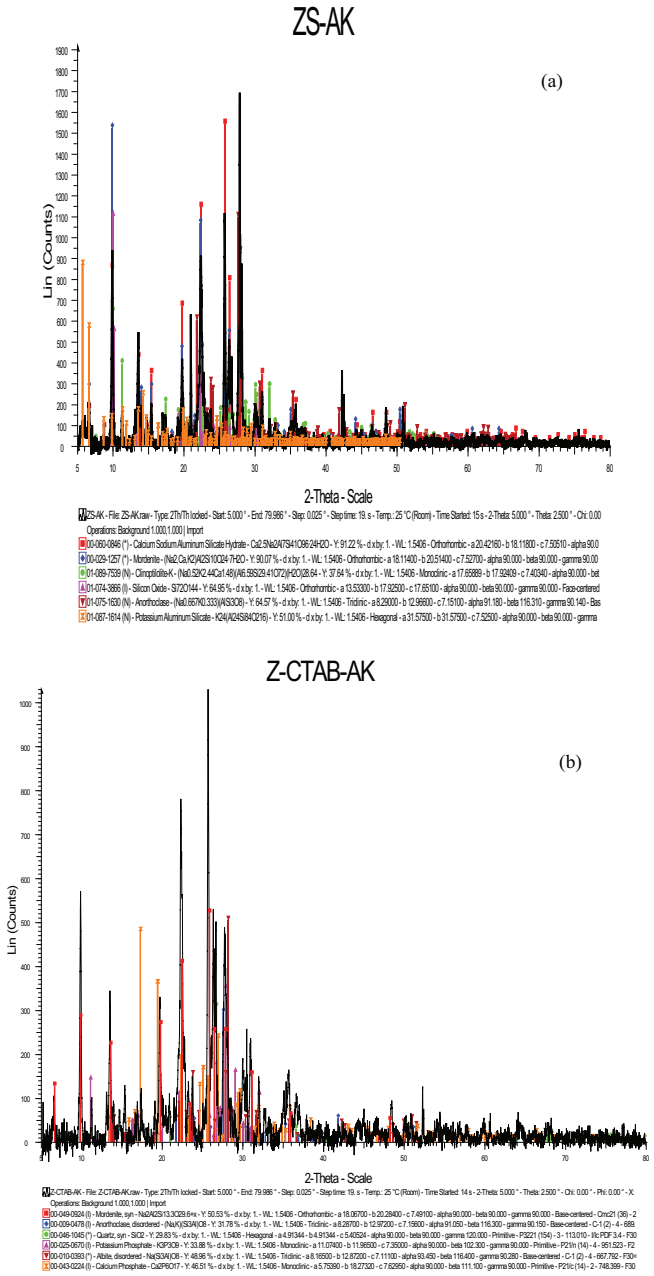

Fig. 6. (a) XRD pattern of Zeolite and (b) Zeolite-CTAB.

4.2. Effect of modification and adsorbent dosage on AB25 adsorption

From Fig. 8, the adsorption capacities of anionic dye by natural zeolite were found to be negative. Due to this reason, the unmodified material adsorbs less amount of dye. Since, the adsorption of small water molecules was adsorbed easily by zeolite microspores, while the large dye molecules are excluded. In the zeolite-CTAB modified the material, zeolite surface modification and covered with the positive charges and increased electrochemical interaction between anionic dye molecules and the zeolite surfaces. Due to this reason, adsorption capacities increased more than four times.

The effect of adsorbent dosage on the adsorption of AB25 on zeolite and zeolite-CTAB from aqueous solution is shown in Fig. 8. Fig. 8, shows that the removal of AB25 by zeolite-CTAB increases up to a certain limit (50 mg) and then it remains almost constant. An increase in adsorption with an increase in adsorbent dose can be attributed to the increased surface area and the availability of more adsorption sites [23]. But the amount adsorbed for a unit mass of the adsorbent decrease considerably. The decrease in unit adsorption with increasing dose of adsorbent is basically due to adsorption sites remaining unsaturated during the adsorption process. For the quantitative removal of AB25 from 25 mL of 50 mg/L a maximum dose of 50 mg of adsorbent is required. Similar behavior has been observed for humic acid (HA) removal by another adsorbent such as acid-activated Greek bentonite [24].

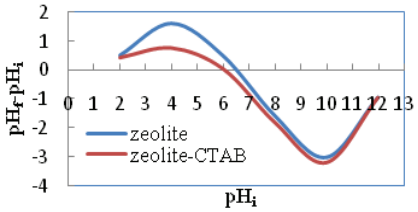

Fig. 7. Determination of the point of zero charge.

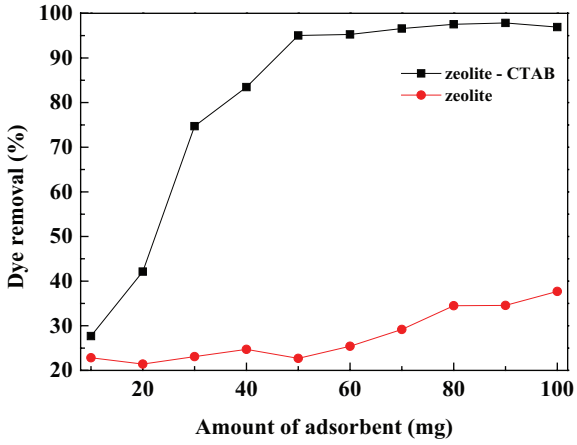

Fig. 8. Effect of adsorbent dosage on the removal percentage of AB25 by using zeolite and zeolite-CTAB. At AB25 concentration: 50 mg/L; Zeolite and zeolite-CTAB doses: 10–100 mg; pH: 6.5; temperature: 25°C ± 1°C; equilibration time: 120 min; rotary speed: 200 rpm.

4.3. Effect of initial pH concentration

The effect of solution pH on the adsorption of AB25 on zeolite and zeolite-CTAB has been investigated in the pH range 2–12, and the results are shown in Fig. 9. It can be shown that the influence of pH strongly influenced the adsorption capacity of AB25. The removal efficiency of AB25 decreases with an increase in pH of the solution. The highest removal efficiency has been achieved at pH 2, and thereafter the removal efficiency has been decreased. Low pH leads to an increase in H^+ ion concentration in the system and the surface of the zeolite acquires positive charge by adsorbing H^+ ions. As the zeolite surface gain positive charge at low pH, a significantly strong electrostatic attraction appears between the sites. There were no significant changes in the pH ranging from 4 to 8 for zeolite-CTAB and 4 to 6 for zeolite. The minor decrease in adsorption with an increase in pH may be attributed to the repulsion between the anionic dye molecules and the abundance of OH^- ions at higher pH values. These results also confirmed with the $pH_{pzc.}$ After pH_{pzc} value, the materials have more negative charge, due to this reason at higher pH decrease in adsorption amount. A similar result was observed for the adsorption of Congo red from aqueous solution onto calcium-rich fly ash [25].

4.4. Effect of initial AB25 concentration and contact time

The adsorption of AB25 on zeolite and zeolite-CTAB has been experimentally investigated at different AB25 concentrations (50–125 mg/L for zeolite-CTAB and 25–100 mg/L for zeolite) and contact time. The results are shown in Figs. 10(a) and (b) for zeolite and zeolite-CTAB, respectively. It was observed that the uptake was rapid for the first 5 min and after that attains saturation both for zeolite and zeolite-CTAB. An increase in initial AB25 concentration results in an increase in the adsorption of AB25 on zeolite and zeolite-CTAB. The equilibrium adsorption for zeolite-CTAB increases from 25 to 50 mg/g with an increase in the initial AB25 concentration from 50 to 125 mg/L and the equilibrium adsorption for zeolite increases from 10 to 39 mg/g with an increase in the initial AB25 concentration from 25 to 100 mg/L. As the initial AB25 concentration increased from 50 to 125 mg/L for zeolite-CTAB, the equilibrium removal registered a decrease from 99.3% to 82.5%. The adsorption rate was very high at early adsorption period due to the availability of a large number of the vacant site which increases the concentration gradient between the adsorbate in the solution and adsorbate on the adsorbent surface [26].

4.5 Adsorption kinetics

For evaluating the adsorption kinetics of AB25, the PFO, and PSO kinetic models have been used to fit the experimental data. A $\log(q_e - q_t)$ vs. t has been plotted for different AB25 concentrations using (3) and (4) (figures are not shown). The values of the kinetic model's constants obtained for the adsorption of AB25 onto zeolite and zeolite-CTAB are summarized in Table 3. The low R^2 values and the difference between $q_{e,exp'}$ and $q_{e,cal}$ indicate that the PFO model was not well fitted to describe the adsorption of AB25 by zeolite and zeolite-CTAB. It may be explained that the PFO model does not fit well to the whole range of contact time and generally underestimate the q_e values.

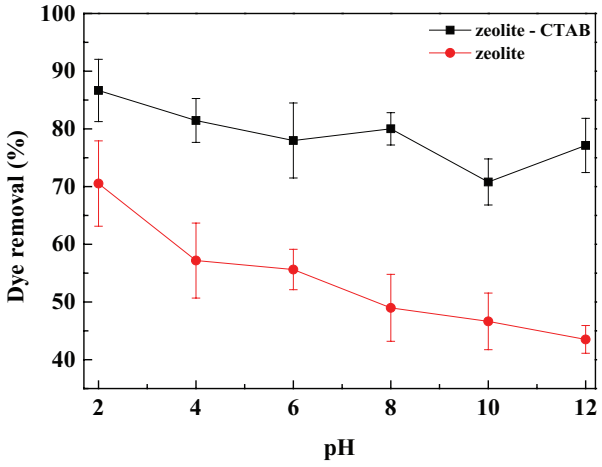

Fig. 9. Effect of pH on equilibrium uptake of AB25. At AB25 concentration: 100 mg/L; Zeolite and zeolite-CTAB doses: 50 mg; pH range: 2–12; temperature: 25°C ± 1°C; equilibration time: 120 min rotary speed: 200 rpm.

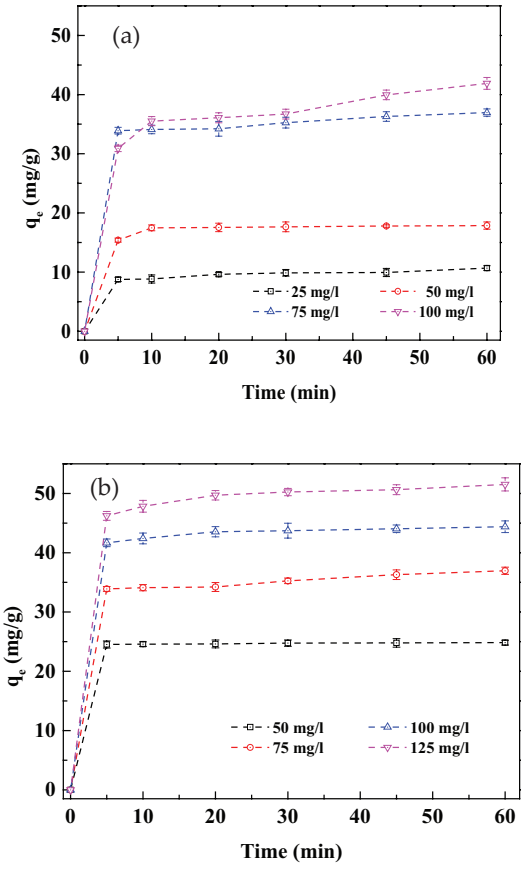

Fig.10. Effect of initial AB25 concentration and contact time on (a) Zeolite. (b) Zeolite-CTAB. (Dosage of adsorbent: 50 mg; pH: 2; time intervals: 5–60 min; rotary speed: 200 rpm; temperature: 25°C ± 1°C and initial concentration: 25–125 mg/L; solution volume 25 mL).

Table 3
Estimated PFO and PSO models rate constants for zeolite and zeolite-CTAB

Zeolite-CTAB	50 mg/L	75 mg/L	100 mg/L	125 mg/L
$q_t = k_2 q_e^2 t/(1 + q_e k_2 t)$				
$q_{e,exp}$	24.8	36.961	44.3828	51.5312
q_e (mg/g)	24.8	36.131	44.337	51.393
k_2 (g/mg.min)	0.62	0.066	0.065	0.032
R^2	0.999	0.997	0.999	0.999
SE	0.06	0.84	0.26	0.45
NSD	0.001	0.05	0.003	0.006
ARE	–0.001	–0.05	–0.002	–0.01
$Q = q_e(1 - \exp(-k_1 t))$				
q_e (mg/g)	24.8	35.4	43.7	50.1
k_1 (1/min)	4.06	0.62	0.61	0.50
R^2	0.999	0.994	0.999	0.997
SE	0.13	1.12	0.64	1.12
NSD	0.003	0.10	0.02	0.04
ARE	–0.002	–0.08	–0.02	–0.03
Zeolite	25 mg/L	50 mg/L	75 mg/L	100 mg/L
$q_t = k_2 q_e^2 t/(1 + q_e k_2 t)$				
$q_{e,exp}$	9.62	17.9	23.7	40.0
q_e (mg/g)	10.3	18.2	36.1	40.9
k_2 (g/mg.min)	0.09	0.07	0.07	0.01
R^2	0.992	0.998	0.997	0.990
SE	0.36	0.31	0.84	1.50
NSD	0.12	0.04	0.05	0.12
ARE	–0.09	–0.04	–0.05	–0.10
$q = q_e(1 - \exp(-k_1 t))$				
q_e (mg/g)	9.87	17.3	35.4	38.5
k_1 (1/min)	0.40	4.06	0.62	0.31
R^2	0.982	0.983	0.994	0.980
SE	0.55	0.94	1.12	2.20
NSD	0.25	0.32	0.10	0.23
ARE	–0.21	–0.27	–0.08	–0.20

Note: Dosage of adsorbent: 50 mg; pH: 2; time intervals: 5–60 min; rotary speed: 200 rpm; temperature: 25°C±1°C and initial concentration: 25–125 mg/L; solution volume; 25 mL.
q; adsorbed AB25 (mg/g) at time *t* (min).

In addition, the R^2 values for the PSO model were relatively higher than that of PFO model values. Moreover, the q_2 values calculated by the PSO model were close to the $q_{e,exp}$ values. The adsorption coefficients of determination (>0.99) were obtained for the PSO kinetic model in zeolite and zeolite-CTAB and its reveals that the sorption process more suitable to this model. This implies that the adsorption best fitted to the PSO model at different initial AB25 concentrations. Similar results for the adsorption of acid dyes have also been reported by other researchers [27,28]. Generally, the higher correlation coefficient (R^2) exhibits a better fit for the model. Statistical analysis for the adsorption kinetics was also carried out utilizing some predictive test tools such as standard error (SE), average relative error (ARE) and normalization standard deviation (NSD) as shown in Table 2. From Table 2, the PSO model was noticed that was statistically conspicuous based on the higher R^2 values and lower SE, NSD, and ARE values compared with PFO model.

4.6. Adsorption isotherms

To determine the AB25 dye adsorption process, the obtained experimental data were analyzed with two most commonly used isotherms models. It was very useful for the determination of the best correlation for the equilibrium curves. In the present study, Langmuir and Freundlich models have been used to analyze the data which are widely used in solid-liquid adsorption systems.

The details of the Langmuir and Freundlich isotherms are given in (5), (7). Figs. 11 and 12 show the adsorption isotherm curves and the obtained values are shown in Table 4. The adsorption isotherms of AB25 onto zeolite and zeolite-CTAB were performed at 30°C–60°C. The results indicated that the amount of adsorbed AB25 increasing compared with natural zeolite. Because of CTAB increase the sorption capacity of zeolite, due to increase the alkyl chain with positive head group of CTAB. This lead to be surface can convert to hydrophobic and neutralizes the negative charges on CTAB-zeolite. The adsorption on zeolite-CTAB is a monolayer adsorption [26]. Based on the Langmuir isotherms model, the predicted maximum monolayer AB25 adsorption capacities for zeolite-CTAB were found to be 112.4 mg/g at pH 2 and at 60°C. For the raw zeolite, the adsorption capacity was found to be 64.2 mg/g at pH 2 and 30°C. In the case of unmodified zeolite with increasing temperature, adsorption capacity is decreasing order. due to the repulsion between negative species of material and dye molecule $–SO_3$ groups. The results show that the correlation coefficient of Langmuir isotherms was higher than that of Freundlich isotherms, indicating that the adsorption of AB25 onto zeolite and zeolite-CTAB can be better fitted with the Langmuir model. The favorability and the nature of the adsorption process can be identified from the value of 1/*n*. In the present study, the value of 1/*n* in raw zeolite and zeolite-CTAB cases is less than one, it is indicating that the adsorption process is favorable. The higher '*n*' value is confirmed the zeolite having heterogeneous nature and reversible adsorption and it is not restricted to the formation of monolayer. However, in the case of zeolite-CTAB the surfactant positive head covered with negative spices. So, in the case of zeolite-CTAB materials adsorption is a monolayer process. The cationic surfactant produces the positive charge on the surface of zeolite. This positive charge and dye molecule SO_3^- interact with each other and due to this mechanism adsorption capacity is very high in zeolite-CTAB compare with zeolite [29]. In another hand, the '*n*' value is less than one in all cases. It indicates that the adsorption of AB25 was more favorable on zeolite-CTAB.

The R_L value is dimensionless constant; it is used to determine the adsorption processes is favorable or not. The R_L value in the present study lies between zero and one indicating that adsorption of AB25 on zeolite and zeolite-CTAB were favorable. To confirm the superiority of fit attained by the adsorption isotherms for AB25 onto zeolite and zeolite-CTAB

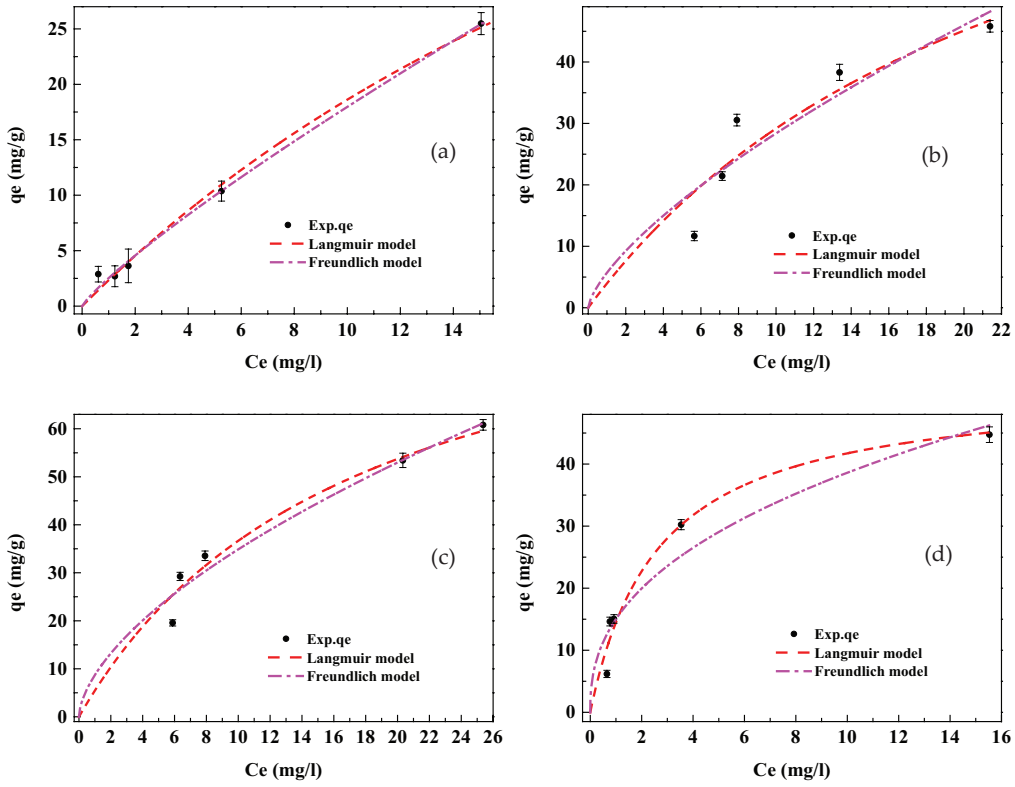

Fig. 11. Langmuir and Freundlich model isotherm plots for AB25 removal at different temperature (a) 30°C, (b) 40°C, (c) 50°C, and (d) 60°C using – Zeolite. Dosage of adsorbent: 50 mg; pH: 2; equilibration time: 60 min; rotary speed: 200 rpm; temperature: 30°C–60°C and initial concentration: 25–100 mg/L (Solution volume: 25 mL).

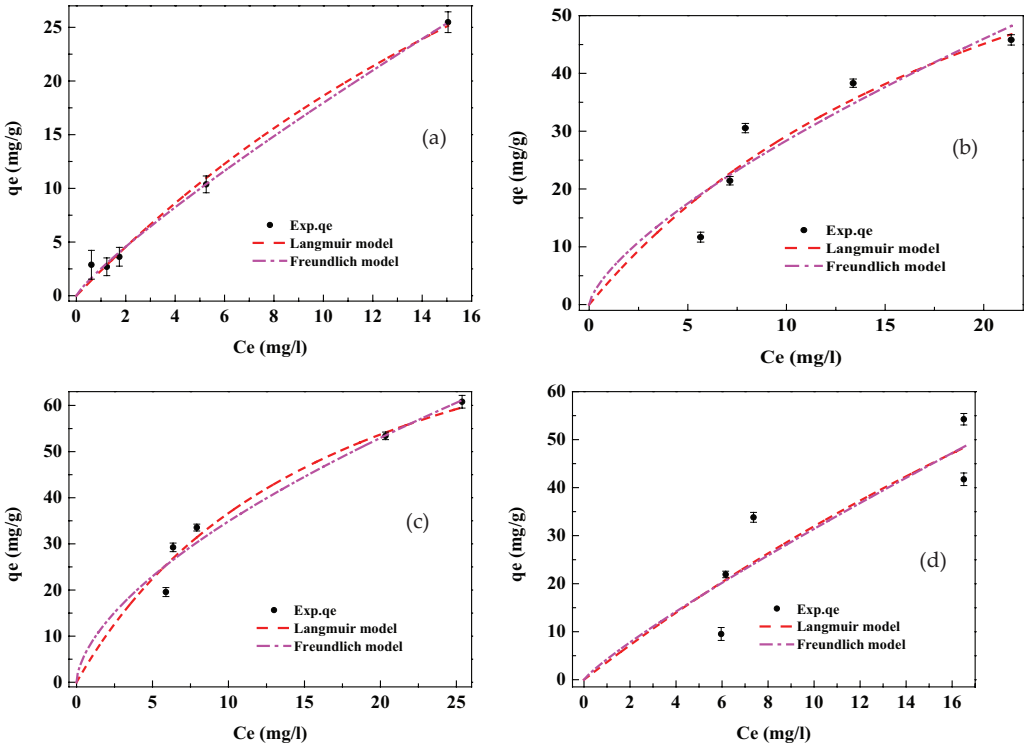

Fig. 12. Langmuir and Freundlich model isotherm plots for AB25 removal at different temperature (a) 30°C, (b) 40°C, (c) 50°C, and (d) 60°C using Zeolite-CTAB (Dosage of adsorbent: 50 mg; pH: 2; equilibration time: 60 min; rotary speed: 200 rpm; temperature: 30°C–60 °C and initial concentration: 50–125 mg/L; solution volume: 25 mL).

adsorbents, different error functions with the correlation coefficient (R^2) were defined. Nonlinear regression was used based on its convergence criteria to minimize the error distribution between the experimental data and the predicted isotherms models. The data analysis demonstrated using excel-solver software, standard error (SE), nonlinear chi-square test (χ^2) and root mean square error (RMSE) is shown in Table 4. The result shows that the lowest value of SE, χ^2, and RMSE with higher values of R^2 for Langmuir model in the corresponding experimental data indicates that the Langmuir isotherm model provided the best fit to the experimental data.

Table 4
Estimated isotherm parameters for AB25 adsorption using Zeolite and Zeolite CTAB at different temperatures

	30°C	40°C	50°C	60°C
Zeolite				
$Q = K_f C_e^{1/n}$				
K_f(mg/g (L/mg)$^{1/n}$)	24.9	19.3	15.8	15.0
1/n	0.33	0.38	0.40	0. 41
R^2	0.925	0.781	0.769	0.925
SE	5.18	8.58	8.44	4.83
RMSE	4.59	7.43	7.31	4.18
χ^2	3.20	8.64	11.2	4.42
$Q = K_L q_m C_e/(1 + K_L C_e)$				
K_L (L/mg)	0.59	0.38	0.36	0.38
q_m (mg/g)	64.2	58.0	54.7	52.8
R^2	0.970	0.907	0.851	0.971
SE	2.80	3.02	6.79	3.03
RMSE	2.89	4.86	5.88	2.62
χ^2	0.99	4.41	7.95	2.50
R_{L1}	0.06–0.01	0.09–0.02	0.10–0.02	0.10–0.02
Zeolite-CTAB				
$q = K_f C_e^{1/n}$				
K_f(mg/g (L/mg)$^{1/n}$)	2.53	5.71	8.70	5.37
1/n	0.85	0.70	0.60	0.84
R^2	0.995	0.842	0.957	0.905
SE	0.77	6.20	4.14	5.43
RMSE	0.67	5.37	3.58	4.71
χ^2	0.98	5.10	1.94	2.35
$Q = K_L q_m C_e/(1 + K_L C_e)$				
K_L (L/mg)	0.03	0.04	0.06	0.05
q_m (mg/g)	82.2	99.4	101	112
R^2	0.993	0.865	0.961	0.925
SE	0.95	5.71	3.92	4.83
RMSE	0.82	6.74	3.40	4.19
χ^2	1.52	7.93	1.73	2.46
R_{L1}	0.58–0.21	0.49–0.16	0.45–0.14	0.41–0.12

Note: Dosage of adsorbent: 50 mg; pH: 2; equilibration time: 60 min; rotary speed: 200 rpm; temperature: 30°C–60°C and initial concentration: 25–125 mg/L; solution volume: 25 mL.

4.7. Thermodynamic study

Temperature is one of the key parameters to achieve knowledge of the thermal character of the adsorption process. The variation of dye removal efficiency concerning the temperature can be explained by various thermodynamic parameters such as $\Delta G°$, $\Delta H°$, and $\Delta S°$, which are evaluated from (8–11). The values of $\Delta H°$ and $\Delta S°$ are obtained from the slope and intercept of a line plotted by $\ln K_d$ vs. $1/T$, respectively. The obtained thermodynamic parameters for the adsorption of AB25 on zeolite-CTAB are presented in Table 5. The increase in AB25 adsorption on zeolite-CTAB was observed with an increase in temperature. This increase in AB25 adsorption on zeolite-CTAB indicates that the preferential adsorption may occur at high temperature [28].

It is evident from the results that the overall the value of the $\Delta G°$ was negative for zeolite-CTAB. The negative value of values of $\Delta G°$ indicates, the adsorption of AB25 is a degree of spontaneous process and thermodynamically favorable at various temperatures. The $\Delta G°$ values increase with temperature for zeolite-CTAB shows the decrease of spontaneous influence. Also, the values of ΔG^0 were less than 60 KJ/mole confirm the adsorption of the AB25 on the zeolite-CTAB was the physical sorption processes. The positive value of enthalpy ($\Delta H°$) indicates the process was endothermic nature and the more interaction of the zeolite-CTAB with AB25. The value of ΔS^0 was found to be positive establish the increasing randomness in the solid-liquid interface interaction during the adsorption process [28].

5. Comparison of zeolite and zeolite-CTAB with other sorbents for the sorption of AB25

The adsorption capacity of zeolite and zeolite-CTAB for the removal of AB25 is shown in Table 6. The adsorption capacity of various, adsorbents for the removal of AB25 is also shown in Table 6. For comparison purpose, the removal capacity of zeolite and zeolite-CTAB compares well, with that of the other adsorbents used. The adsorption capacity of zeolite and zeolite-CTAB for AB25 was found to be 64.2 and 112.4 mg/g, respectively. The zeolite-CTAB shows the higher adsorption capacity than various low-cost adsorbents for AB25, reported in the literature. It can be concluded that zeolite-CTAB was extremely effective in the removal of AB25 from aqueous solution when compared with the effectiveness of other adsorbents [4,30,31–37]. However, the adsorption capacities of zeolite and zeolite-CTAB for removal

Table 5
Thermodynamic parameters for AB25 adsorption on Zeolite-CTAB at four different temperatures

Temperature (°C)	$\Delta G°$ (kJ/mol)	$\Delta H°$ (kJ/mol)	$\Delta S°$ (kJ/mol. K)
30	–23.7	18.1	0.14
40	–25.4		
50	–27.1		
60	–27.7		

Note: Dosage of adsorbent: 50 mg; pH: 2; equilibration time: 60 min; rotary speed: 200 rpm; temperature: 30°C–60°C and initial concentration: 50–125 mg/L; solution volume: 25 mL.

Table 6
Comparison of zeolite and zeolite-CTAB with other sorbents for the sorption of AB25

S. No.	Adsorbent	Q_{max} (mg/g)	Reference
1	Wood sawdust (raw)	5.92	[30]
2	Peat	12.7	[31]
3	Baggase pith	17.5	[32]
4	Diatomite	21.4	[33]
5	Spent brewery grains	24.0	[34]
6	Saw dust-pitch pine	26.2	[35]
7	Saw dust-oak	27.9	[35]
8	Saw dust-cherry	31.9	[35]
9	Saw dust-walnut	36.9	[35]
10	Indian jujuba seed powder (IJSP)	54.9	[4]
11	Hazelnut shell	60.2	[35]
12	Natural sepiolite	39.3–87.5	[36]
13	Unmodified and Cetylpyridinium chloride (CPC)-modified biomass of Penicillium (P.YW 01)	74.4–90.4	[37]
14	Waste tea activated carbon	203	[38]
15	Cationized starch-based material	322	[39]
16	Zeolite	64.2	Present study
17	Zeolite-CTAB	112	Present study

of AB25 are less than those reported for waste tea activated carbon [38] and cationized starch-based material [39]. This is due to the fact that the initial concentrations of AB25 used in these studies were higher than 50–125 mg/L.

6. Conclusion

The present study revealed that surfactant modified zeolite; zeolite-CTAB acts a well adsorbent for the removal of acidic dye AB25 from aqueous solutions. Zeolite-CTAB adsorption capacity is higher than zeolite. The FT-IR, SEM, and EDX show that the modification of zeolite with CTAB was successful. The XRF study shows that the macro-pores on the surface of adsorbents are filled up by CTAB molecules after modification. It is also eluded in FT-IR, SEM and EDX analysis that dye was loaded on the adsorbent surface. Kinetics study shows that the adsorption reaction follows the PSO kinetic model ($R^2 > 0.99$). In both cases, the adsorption processes completely depend on the pH. The highest removal efficiency has been achieved at around pH 2, and after that the removal efficiency was decreased. From the initial dye concentration and contact time, it was clear that the adsorption rate was very high at early adsorption period due to the availability of a large number of the vacant site which increases the concentration gradient between the adsorbate in the solution and adsorbate on the adsorbent surface. The maximum adsorption capacity for zeolite-CTAB and zeolite are found to be 112 and 64.2 mg/g, respectively. The equilibrium data were found to be well represented by the Langmuir model for zeolite-CTAB and zeolite. The R_L values in the present study lies between zero and one that indicate the adsorption of AB25 on zeolite-CTAB and zeolite were favorable. In the present study, the value of n in all cases was greater than one indicating that the adsorption process is favorable. The results corroborate that the positive value of $\Delta H°$ indicating the adsorption processes was endothermic and decreasing the $\Delta G°$ with increasing temperature was obvious indicators of the endothermic character for the AB25 adsorption onto the zeolite-CTAB adsorbent. The positive $\Delta S°$ value shows increasing irregularity within the solution/adsorbent during the adsorption of the dye AB25. The zeolite-CTAB containing amino-group, it will be useful to attract of anionic organic dye pollutants from dye-containing wastewater.

Acknowledgments

The author L. Sivarama Krishna is grateful to the Graduate School and The Thailand Research Fund (IRG578001), Chulalongkorn University for providing financial support, Postdoctoral Fellowship under Rachadapisaek Sompote Fund. The author Mohammad Alamgir Kabir is grateful to the Government of the Peoples' Republic of Bangladesh for the financial assistance through the STREC project (Strengthening the Research and Exploration Capabilities of the Geological Survey of Bangladesh). The authors also express their deepest gratitude to the authorities of the University Kebangsaan Malaysia (UKM) to organize this program.

References

[1] G. Moussavi, R. Khosravi, The removal of cationic dyes from aqueous solutions by adsorption onto pistachio hull waste, Chem. Eng. Res. Des., 89 (2011) 2182–2189.
[2] M. Anbia, S.A. Hariri, Removal of methylene blue from aqueous solution using nanoporous SBA-3, Desalination, 261 (2010) 61–66.
[3] E. Bulut, M. Özacar, İ.A. Şengil, Equilibrium and kinetic data and process design for adsorption of Congo Red onto bentonite, J. Hazard. Mater., 154 (2008) 613–622.
[4] L.S. Krishna, A.S. Reddy, W.Y.W. Zuhairi, M.R. Taha, A.V. Reddy, Indian jujuba seed powder as an eco-friendly and a low-cost biosorbent for removal of Acid Blue 25 from aqueous solution, Sci. World J., 2014 (2014) 11.

[5] M. Tuzen, A. Sarı, T.A. Saleh, Response surface optimization, kinetic and thermodynamic studies for effective removal of rhodamine B by magnetic AC/CeO_2 nanocomposite, J. Environ. Manage., 206 (2018) 170–177.
[6] E. Altıntıg, H. Altundag, M. Tuzen, A. Sarı, Effective removal of methylene blue from aqueous solutions using magnetic loaded activated carbon as novel adsorbent, Chem. Eng. Res. Des., 122 (2017) 151–163.
[7] L. Sivarama Krishna, A. Sreenath Reddy, A. Muralikrishna, W.Y. Wan Zuhairi, H. Osman, A. Varada Reddy, Utilization of the agricultural waste (Cicer arientinum Linn fruit shell biomass) as biosorbent for decolorization of Congo red, Desal. Wat. Treat., 56 (2015) 2181–2192.
[8] L.S. Krishna, A. Yuzir, G. Yuvaraja, V.A. Kumar, Removal of Acid blue25 from aqueous solutions by using Bengal gram fruit shell (BGFS) biomass, Int. J. Phytorem., 19 (2016) 431–438.
[9] K-C. Chen, J-Y. Wu, C-C. Huang, Y-M. Liang, S-C.J. Hwang, Decolorization of azo dye using PVA-immobilized microorganisms, J. Biotechnol., 101 (2003) 241–252.
[10] K. Singh, S. Arora, Removal of synthetic textile dyes from wastewaters: a critical review on present treatment technologies, Crit. Rev. Env. Sci. Technol., 41 (2011) 807–878.
[11] O.S. Bello, K.A. Adegoke, A.A. Olaniyan, H. Abdulazeez, Dye adsorption using biomass wastes and natural adsorbents: overview and future prospects, Desal. Wat. Treat., 53 (2015) 1292–1315.
[12] M.C.S. Reddy, L. Sivaramakrishna, A.V. Reddy, The use of an agricultural waste material, Jujuba seeds for the removal of anionic dye (Congo red) from aqueous medium, J. Hazard. Mater., 203 (2012) 118–127.
[13] H. Ghobarkar, O. Schäf, U. Guth, Zeolites—from kitchen to space, Prog. Solid State Chem., 27 (1999) 29–73.
[14] L.D.T. Prola, F.M. Machado, C.P. Bergmann, Adsorption of Direct Blue 53 dye from aqueous solutions by multi-walled carbon nanotubes and activated carbon, J. Environ. Manage., 130 (2013) 166–175.
[15] K.V. Kumar, Linear and non-linear regression analysis for the sorption kinetics of methylene blue onto activated carbon, J. Hazard. Mater., 137 (2006) 1538–1544.
[16] I. Langmuir, The constitution and fundamental properties of solids and liquids, J. American Chem.Soci., 38 (1916) 2221–2295.
[17] H.M.F. Freundlich, Over the adsorption in solution, J. Phys. Chem., 57 (1906) 385–471.
[18] N. Bektaş, S. Aydın, M.S. Öncel, The Adsorption of arsenic ions using beidellite, zeolite, and sepiolite clays: a study of kinetic, equilibrium and thermodynamics, Sep. Sci. Technol., 46 (2011) 1005–1016.
[19] Y. Liu, Some consideration on the Langmuir isotherm equation, Colloids Surf. A-Physicochem. Eng. Asp., 274 (2006) 34–36.
[20] Y. Liu, Is the free energy change of adsorption correctly calculated?, J. Chem. Eng. Data, 54 (2009) 1981–1985.
[21] A. Özcan, Ç. Ömeroğlu, Y. Erdoğan, A.S. Özcan, Modification of bentonite with a cationic surfactant: an adsorption study of textile dye Reactive Blue 19, J. Hazard. Mater., 140 (2007) 173–179.
[22] J. Lin, Y. Zhan, Adsorption of humic acid from aqueous solution onto unmodified and surfactant-modified chitosan/zeolite composites, Chem. Eng. J., 200–202 (2012) 202–213.
[23] B.H. Hameed, Evaluation of papaya seeds as a novel non-conventional low-cost adsorbent for removal of methylene blue, J. Hazard. Mater., 162 (2009) 939–944.
[24] D. Doulia, C. Leodopoulos, K. Gimouhopoulos, F. Rigas, Adsorption of humic acid on acid-activated Greek bentonite, J. Colloid Interface Sci., 340 (2009) 131–141.
[25] B. Acemioğlu, Adsorption of Congo red from aqueous solution onto calcium-rich fly ash, J. Colloid Interface Sci., 274 (2004) 371–379.
[26] B. Zohra, K. Aicha, S. Fatima, B. Nourredine, D. Zoubir, Adsorption of Direct Red 2 on bentonite modified by cetyltrimethylammonium bromide, Chem. Eng. J., 136 (2008) 295–305.
[27] N. Mirzaei, M. Hadi, M. Gholami, R.F. Fard, M.S. Aminabad, Sorption of acid dye by surfactant modificated natural zeolites, J. Taiwan. Inst. Chem. Eng., 59 (2016) 186–194.
[28] X. Jin, B. Yu, Z. Chen, J.M. Arocena, R.W. Thring, Adsorption of Orange II dye in aqueous solution onto surfactant-coated zeolite: characterization, kinetic and thermodynamic studies, J. Colloid Interface Sci., 435 (2014) 15–20.
[29] H-P. Chao, S-H. Chen, Adsorption characteristics of both cationic and oxyanionic metal ions on hexadecyltrimethylammonium bromide-modified NaY zeolite, Chem. Eng. J., 193–194 (2012) 283–289.
[30] Y-S. Ho, G. McKay, Kinetic models for the sorption of dye from aqueous solution by wood, Process Saf. Environ. Prot., 76 (1998) 183–191.
[31] Y.S. Ho, G. McKay, Sorption of dye from aqueous solution by peat, Chem. Eng. J., 70 (1998) 115–124.
[32] B. Chen, C.W. Hui, G. McKay, Film-pore diffusion modeling and contact time optimization for the adsorption of dyestuffs on pith, Chem. Eng. J., 84 (2001) 77–94.
[33] K. Badii, F.D. Ardejani, M.A. Saberi, N.Y. Limaee, S. Shafaei, Adsorption of Acid blue 25 dye on diatomite in aqueous solutions, Indian J. Chem. Technol., 17 (2010) 7–16.
[34] V. Jaikumar, K.S. Kumar, D.G. Prakash, Biosorption of acid dyes using spent brewery grains: characterization and modeling, Int. J. App. Sci. Eng., 7 (2009) 115125.
[35] F. Ferrero, Dye removal by low cost adsorbents: hazelnut shells in comparison with wood sawdust, J. Hazard. Mater., 142 (2007) 144–152.
[36] Z-X. Han, Z. Zhu, D-D. Wu, J. Wu, Y-R. Liu, Adsorption kinetics and thermodynamics of Acid Blue 25 and Methylene Blue dye solutions on natural sepiolite, Synth. React. Inorg. M., 44 (2014) 140–147.
[37] Y. Yang, D. Jin, G. Wang, D. Liu, X. Jia, Y. Zhao, Biosorption of Acid Blue 25 by unmodified and CPC-modified biomass of Penicillium YW01: kinetic study, equilibrium isotherm and FTIR analysis, Colloids Surf., B., 88 (2011) 521–526.
[38] M. Auta, B.H. Hameed, Preparation of waste tea activated carbon using potassium acetate as an activating agent for adsorption of Acid Blue 25 dye, Chem. Eng. J., 171 (2011) 502–509.
[39] F. Renault, N. Morin-Crini, F. Gimbert, Cationized starch-based material as a new ionexchanger adsorbent for the removal of C.I. Acid Blue 25 from aqueous solutions, Biores. Technol., 99 (2008) 7573–7586.